LETTER

Minnealloy: a new magnetic material with high saturation flux density and low magnetic anisotropy

Letters

IOP Publishing

Journal of Physics D: Applied Physics

J. Phys. D: Appl. Phys. **50** (2017) 37LT01 (6pp)

https://doi.org/10.1088/1361-6463/aa8130

Letter

Minnealloy: a new magnetic material with high saturation flux density and low magnetic anisotropy

Md Mehedi[1,3], Yanfeng Jiang[2,3], Pranav Kumar Suri[1], David J Flannigan[1] and Jian-Ping Wang[2,4]

[1] Department of Chemical Engineering and Materials Science, University of Minnesota Twin Cities, Minneapolis, MN, United States of America

[2] Department of Electrical and Computer Engineering, University of Minnesota Twin Cities, Minneapolis, MN, United States of America

E-mail: jpwang@umn.edu

Received 18 April 2017, revised 29 June 2017
Accepted for publication 20 July 2017
Published 22 August 2017

Abstract

We are reporting a new soft magnetic material with high saturation magnetic flux density, and low magnetic anisotropy. The new material is a compound of iron, nitrogen and carbon, α'-$Fe_8(NC)$, which has saturation flux density of 2.8 ± 0.15 T and magnetic anisotropy of 46 kJ m^{-3}. The saturation flux density is 27% higher than pure iron, a widely used soft magnetic material. Soft magnetic materials are very important building blocks of motors, generators, inductors, transformers, sensors and write heads of hard disk. The new material will help in the miniaturization and efficiency increment of the next generation of electronic devices.

Keywords: magnetic materials, high saturation flux density, minnealloy, soft magnetic materials, high saturation magnetization

Supplementary material for this article is available online

(Some figures may appear in colour only in the online journal)

1. Introduction

Soft magnetic material is an important building block for motors, generators, sensors, write heads of hard disk drives, transformers, and inductors [1–4]. A combination of high saturation flux density, and low magnetic anisotropy is rare to find in one soft magnetic material. The high saturation flux density will enable the reduction of machine size, and low magnetic anisotropy will enable higher efficiency [5]. With this combination, the material can be used as the core in high efficiency energy converter applications. Moreover, the fast growth of areal density of magnetic recording media requires a high flux density material with low magnetic anisotropy for write heads [6]. Currently available soft magnetic materials such as Fe, Fe–Ni, Fe–Si, Fe–Co, ferrites and Fe-based nanocrystalline and amorphous soft magnets cannot provide this desired combination [7–17]. Silicon steel (Fe–Si), pure iron (Fe), Permalloy (Fe–Ni), and nanocrytalline and amorphous Fe-based alloys [18], which are currently used in high performance transformers and motors, have saturation flux density of 1.3–2.2 T [9, 13, 18]. The Fe–Co alloy, which is currently used in write heads, has a higher saturation flux density of 2.40 T [11, 15, 19], however Co is a 'critical material' based on its supply chain risk reported by the Critical Materials Institute [20]. In the 1990s, α''-$Fe_{16}N_2$ was reported with a flux density of 2.8–3.0 T, which triggered the search for Fe–N

[3] The authors contributed equally.

[4] Author to whom any correspondence should be addressed.
200 Union St SE, 1-165 Keller Hall, Minneapolis, MN 55455, United States of America.

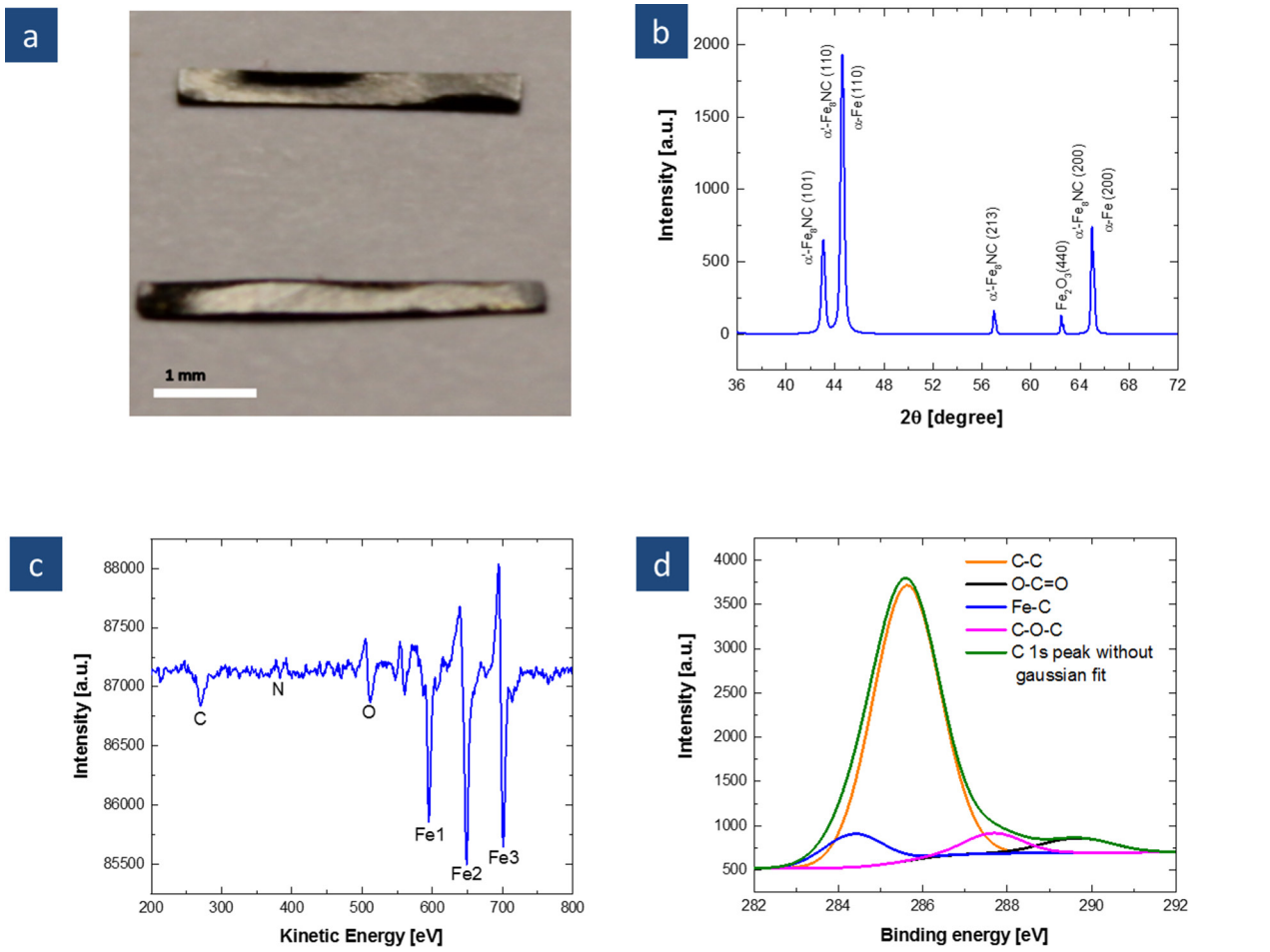

Figure 1. Characterization of the minnealloy sample, (a) Minnealloy ribbon samples. (b) XRD patterns of Minnealloy. (c) AES of Minnealloy sample revealed a mixture of Fe, N, C and O in the sample. (d) The bonding of oxygen and carbon are well understood by doing XPS. The XPS data prove the existence Fe–C bonds.

based high flux density materials [21]. However, α''-$Fe_{16}N_2$ has a high magnetocrystalline anisotropy of 1000 kJ m^{-3} [22, 23], which renders it unsuitable for soft magnetic applications. With increasing demand for machine miniaturization, energy efficiency, and reduction of dependence on elements that are in short supply, much effort is currently devoted to the search of new sustainable materials with a high saturation flux density of >2.4 T, and low coercivity of 5–80 A m^{-1}. Herein, we report a new soft magnetic material, Minnealloy, a compound of Fe, N and C, α'-Fe_8(NC). The superior magnetic fux density of Minnealloy suggests that this material will be helpful in building next-generation electronic systems having smaller size and weight.

2. Materials and methods

The material was prepared by a vacuum cold crucible casting system (Crystalox Bridgman Stockbarger System) which is based on the induction melting process. The vacuum of 2×10^{-2} mbar was obtained using a mechanical pump, and then Ar was used as a working gas. The molten metal was levitated in the water-cooled crucible with the aid of magnetic levitation. Urea (Sigma-Aldrich, 99.5%) was used as the source of nitrogen and carbon and was wrapped inside a

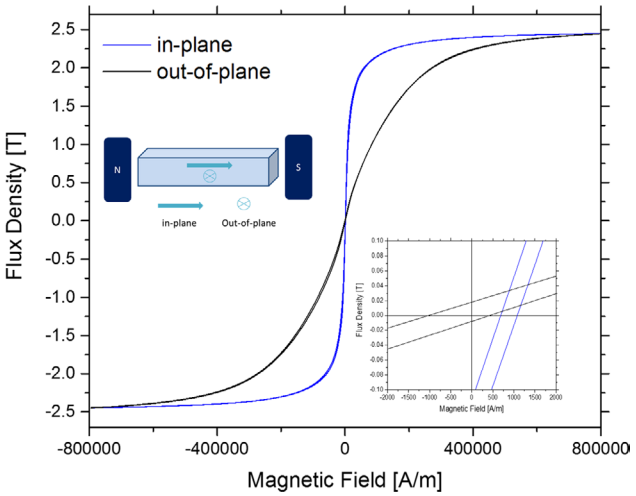

Figure 2. The magnetic properties of the Minnealloy sample. The hysteresis loop of the mixed phase sample with α'-FeN/α'-FeC and α-Fe phase demonstrated a saturation flux density of 2.47 T with 197 A m^{-1} along the in-plane direction of the foil. The coercivity in both direction is zoomed in the inset.

0.1 mm iron foil (Sigma Aldrich, 99.5%). The chemical reaction of decomposition of urea ($(NH_2)_2CO$) was as follows:

$$(NH_2)_2CO = NH_3 + HCNO$$

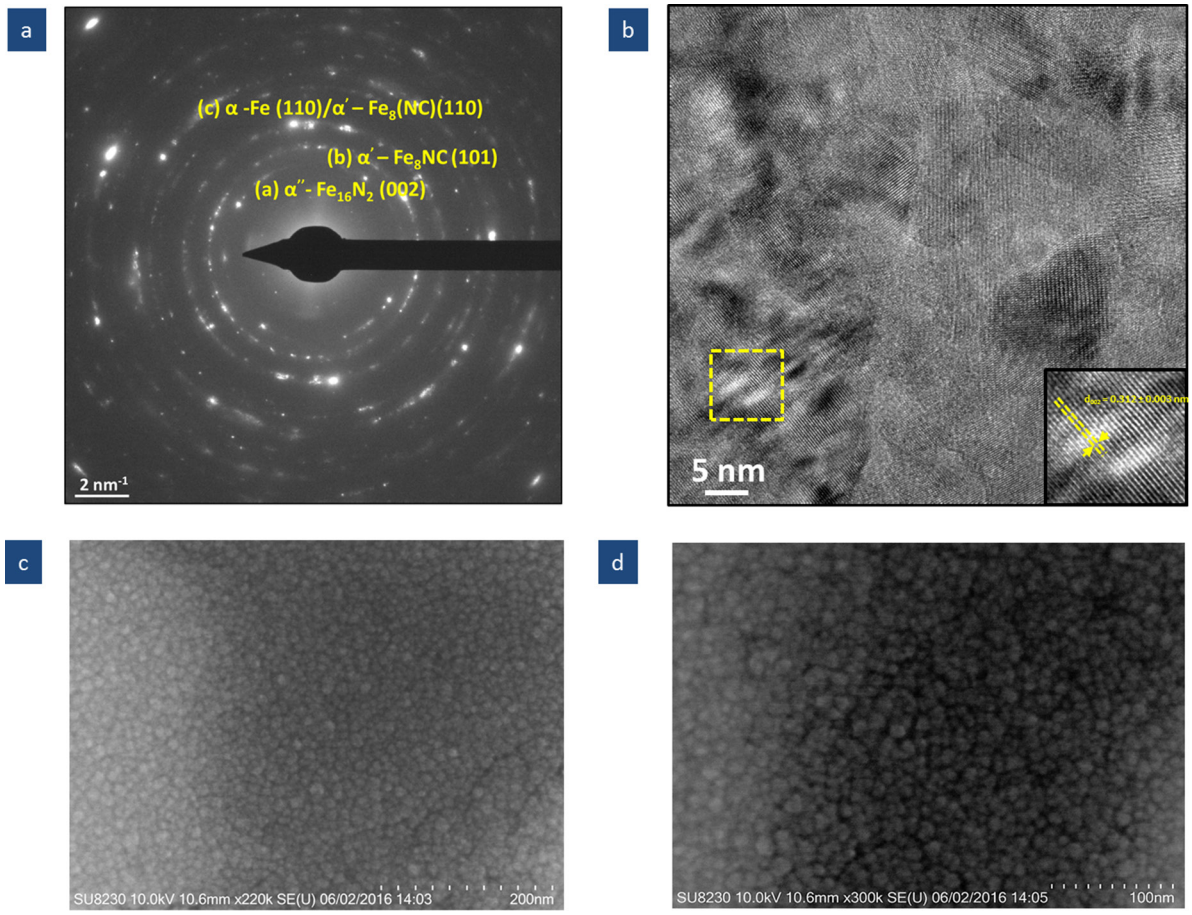

Figure 3. Microstructural characterization via TEM and SEM, (a) SAED pattern showing that the sample is a mixture of α'-$Fe_8(NC)$ and α-Fe. (b) HR-TEM image showing presence of lattice spacing to (0 0 2) planes of ordered BCT iron nitride phase, α''-$Fe_{16}N_2$.

$$2NH_3 \rightarrow 2\,[N] + 3H_2.$$

The wrapped precursor was compressed in a cold press at 2 MPa for 10 min and a pellet-like Fe-urea precursor was prepared. The iron foil was initially melted by induction heating and the decomposed urea (NH_2–CO–NH_2) was the source to diffuse nitrogen and carbon in the molten iron to form γ-FeNC (solid solution of N and C in Fe lattice). The crystal structure of γ-FeNC is face-centered-cubic (FCC), where N and C atoms are randomly distributed in face center positions of Fe lattice. The sphere shaped sample was then cut into ribbons of $5 \times 1 \times 0.2\,mm^3$ size. The ribbons were then annealed at 640 °C for 30 min and quenched in ice-water to transform FCC crystal structure to body center tetragonal crystal structure. After quenching, martensitic α'-$Fe_8(NC)$ was formed, and was annealed at 180 °C for 20 h to remove the residual stress generated in the lattice due to quenching process.

The chemical composition of the sample was measured by Physical Electronics 670 Auger electron spectroscopy (AES). The analysis was done at 5 kV/5 nA. AES measurement was done after removing 1 μm of the surface material via sputtering using Ar gas. Physical Electronics 555 x-ray photoelectron spectroscopy (XPS) (non-monochromatic Mg/Al K-α x-ray source) was used to measure the binding energy of carbon with iron and oxygen. A microdiffractometer with Cu Kα radiation (Bruker D8 Discover 2D) was used to obtain the x-ray diffraction (XRD) spectrum. The spectrum was refined by fitting the data in a Gaussian profile using JADE. The magnetic properties of the sample was measured using a Princeton Measurements vibrating sample magnetometer (VSM) 3900 series, which has a sensitivity of 5×10^{-9} Am^2 (5 μemu). The field resolution of the VSM is 0.5 Oe or, 40 A m^{-1} (0.005% of full range field up to 10 KOe). Before each measurement, the instrument was calibrated using a standard Ni sample with known magnetic moment (44.4 memu), provided by NIST. The density of the sample was calculated by measuring the mass of the sample using Secura225D-1S mass balance system with 0.000 01 g resolution and then, calculated the volume of the ribbon based on the dimensions (width, length and thickness). Scanning electron microscopy was done by using Hitachi SU8230 SEM. Transmission electron microscope (TEM) samples were prepared in an FEI Quanta 200 3D focused ion beam (FIB) operating at 30 kV of gallium ion beam with a lift-out method. FEI Tecnai G2 F30 (S)TEM having a Schottky field emission electron gun operating at 300 kV with extraction voltage of 4 kV was used for electron diffraction and conventional bright-field TEM imaging.

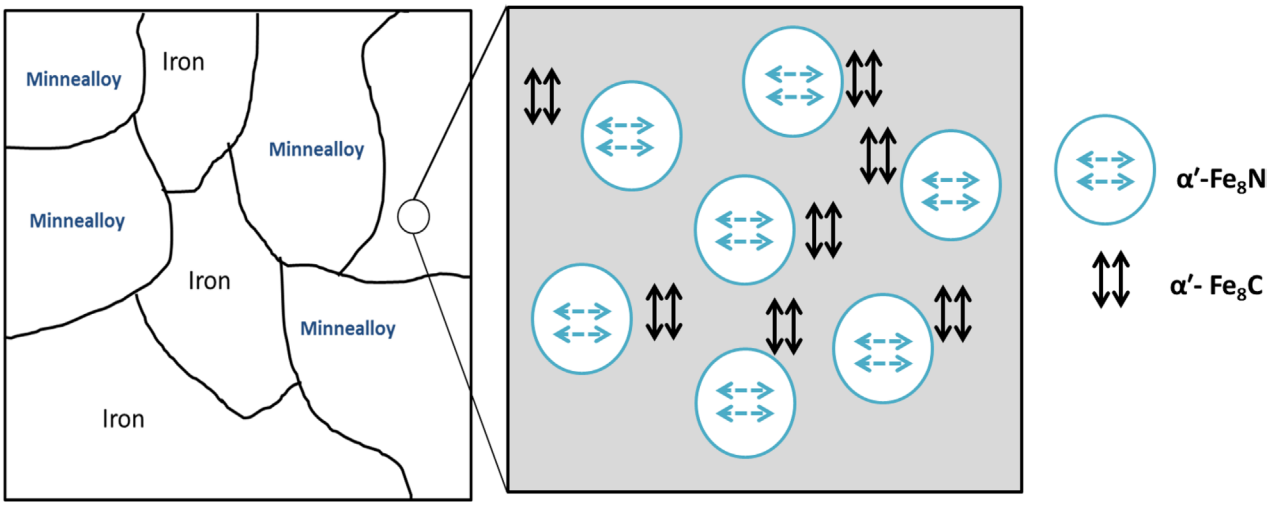

Figure 4. Schematic of the proposed model for obtaining low magnetic anisotropy. (a) The schematic of grain structure of the sample. The sample is a mixture of Minnealloy and pure Fe. The zoomed in view inside a grain is shown in (b). (b) The localized positive and negative anisotropy energy of α'-Fe_8C and α'-Fe_8N with different easy axis direction forms low-anisotropy Minnealloy.

3. Results

The prepared ribbons with a dimension of 3.4–3.9 × 0.35 × 0.2 mm^3 are shown in figure 1(a). XRD of the Minnealloy samples was done with Cu Kα radiation. The $\theta-2\theta$ scan is shown in figure 1(b). The martensitic phase transformation is one of the main controlling factors of the purity of the Minnealloy samples. The Gibbs free energy change (ΔG) of the martensitic phase transformation is proportional to the degree of undercooling below the martensite start temperature. To obtain a high volume percentage of martensite phase, the quenching process was optimized by selecting proper quenching media and quenching time. The XRD $\theta-2\theta$ scan of the quenched sample showed diffraction peaks from the martensite phase, α'. Unique peaks were obtained from the (101), (110), and (200) planes of Minnealloy (α'-Fe_8(NC)). Based on the XRD scan, we found a 42 ± 12% vol α'-Fe_8(NC) phase with a 53 ± 12%vol Fe and a 5 ± 1%vol Fe_2O_3. The calculation of phase composition is shown in supplementary S1 (stacks.iop.org/JPhysD/50/37LT01/mmedia). The lattice parameter was also calculated based on the lattice spacing obtained in XRD. The Minnealloy phase has a lattice parameter of $a = 0.288$ nm and $c = 0.305$ nm.

We analyzed the composition of the sample by AES. The spectrum from the AES is presented in figure 1(c). We found a composition of 71 at% iron, 4 at% nitrogen, 14 at% carbon, and 11 at% oxygen in the Minnealloy sample. The excess carbon is randomly distributed in the Fe lattice, which is evident from the XPS result shown in figure 1(d). In order to understand the carbon distribution, we analyzed the carbon concentration with XPS. Figure 1(d) shows the Gaussian fit of the C 1s spectra, where four peaks are obtained at 284.4, 285.6, 287.7 and 289.6 eV. The peak at 287.7 eV arises from the C–O–C bond [24], while the peaks at 285.6 and 289.6 eV are from the C–C and O–C=O bonds, respectively [25]. Jiang *et al* [25] also observed the evidence of an Fe–C bond from 283.9 to 284.3 eV, which confirms the existence of Fe–C bond in our sample at 284.4 eV. Based on the Gaussian fitting of the plot, 4 at% carbon bonds to iron to form an α'-Fe–C compound. Carbon and oxygen originating from the decomposition of urea (NH_2–CO–NH_2), which are trapped inside the bulk sample due to very fast cooling.

Magnetic properties of the Minnealloy were measured with a VSM with a maximum applied field up to 800 kA m^{-1}. Figure 2 shows the magnetic hysteresis loop of a Minnealloy sample. The ribbon sample with mixed phases possesses a specific saturation magnetization (M_s) of of 258 emu g^{-1} (sample density, $\rho = 7.6 \pm 0.05$ g/cc). The saturation flux density, $B_s = 4\pi M_s\rho/10^4$, was obtained as of 2.47 T, which is demonstrated in figure 2. The saturation flux density of 2.47 T of the ribbon is a mixed contribution from Minnealloy, α-Fe and Fe_2O_3. We calculated the contribution from Minnealloy phase based on the wt% of phases calculated by using XRD scan. The saturation flux density of Minnealloy phase was found as 2.8 ± 0.15 T. Details of the calculation are enclosed in supplementary S2. The coercivities of the sample were 197 A m^{-1} (~2.4 Oe) and 295 A m^{-1} (~3.7 Oe) for the applied magnetic field along the in-plane and out-of-plane direction of the ribbon, respectively. Coercivity is an extrinsic property, which can further be reduced by microstructure engineering with small doping element and heat treatment. Considering the importance of rapid publication of this important finding, we can report a detailed study on microstructure engineering for coercivity reduction in future publications.

4. Discussion

4.1. Magnetic anisotropy

The magnetic anisotropy was calculated based on the law of approach to saturation (LAST) stated in equation (1) [26]:

$$M(H) = M_s\left(1 - \frac{\beta K^2}{M_s^2 H^2}\right), \quad (1)$$

where H is the external magnetic field, $M(H)$ is the magnetization at a specific magnetic field, M_s is the

saturation magnetization of the material, $\beta = 4/15$ for an uniaxial magnetocrystalline anisotropy material, and K is the principal magnetic anisotropy. The magnetocrystalline anisotropy of Minnealloy was found as 46 kJ m^{-3}, which is comparable to the low magnetocrystalline anisotropic material, i.e. α-Fe (45 kJ m^{-3}). Details of the magnetic anisotropy calculation are shown in supplementary S3.

4.2. Microstructure

Figure 3 shows the microstructural characterization of the Minnealloy sample using transmission electron microscopy (TEM) and scanning electron microscopy (SEM). The selected area electron diffraction (SAED) pattern in figure 3(a) reveals that the examined ribbon contains phases such as α'-$Fe_8(NC)$ and α-Fe. The diffraction patterns match to the result found in XRD. Figure 3(b) shows a high-resolution TEM (HR-TEM) image, and corroborates the crystalline structure of Minnealloy. The inset in figure 3(b) illustrates the lattice spacing matching the (0 0 2) planes of α''- $Fe_{16}N_2$, supporting the presence of some ordered Fe–N martensite phases in Minnealloy (supplementary S4). The microstructure of Minnealloy is shown in figures 3(c) and (d). The grain size and shape is quite homogeneous throughout the sample. The average size of the grain is quantified as 16.2 ± 3.8 nm.

The structure and composition characterization methods used here suggest the presence of an α'-$Fe_8(NC)$ phase with some ordered α''-$Fe_{16}N_2$, though other Fe–N and Fe–C phases may be present. Owing to compositional complexity and the importance of rapid reporting of the magnetic results, detailed determination of the structure and composition will be the subject of future work.

4.3. Physical model for low magnetic anisotropy

The theoretical basis of Minnealloy's high saturation flux density and low magnetic anisotropy is not well understood. A physical model is proposed in figure 4. The model depicts a soft magnetic material with two mixed phases, one with positive magnetocrystalline anisotropy, and one with negative magnetocrystalline anisotropy and it can explain the low magnetic anisotropy. α'-Fe_8N and α'-Fe_8C have magnetocrystalline anisotropy of 4.6×10^6 erg cm^{-3}, and -2.1×10^6 erg cm^{-3}, respectively [27–29]. The easy axis of magnetization of the α'- Fe_8N and α'-Fe_8C is along [0 0 1] and [1 0 0], respectively, thus the magnetocrystalline anisotropy has different signs. When the phases are present in a cluster, their magnetocrystalline anisotropy annihilates each other; and we obtain a material with a high saturation flux density, and a low magnetocrystalline anisotropy.

5. Conclusion

In conclusion, the present work demonstrates that we synthesized 'Minnealloy' (α'-$Fe_8(NC)$)-a compound of iron, nitrogen and carbon, with a high saturation flux density, a low magnetic anisotropy and a low coercivity. Saturation flux density is at least 27% higher than α-Fe, and magnetic anisotropy is equivalent to α-Fe. This new soft magnetic material can help greatly in miniaturization of electronic devices, and also can boost the efficiency of the electric systems such as transformers, inductors, hard disk write heads etc.

Acknowledgment

We would like to thank Dr Xiaowei Zhang, Prof Bin Ma, Blake Wolf and Xudong Hang for their valuable discussion. This work was partially supported by ARPA-E (Advanced Research Projects Agency-Energy) project under Contract No. 0472-1595. Part of this work was carried out in the College of Science and Engineering Characterization Facility, University of Minnesota, which has received capital equipment funding from the NSF through the UMN MRSEC program under Award Numbers DMR-0819885 and DMR-1420013.

References

[1] Hamler A, Goričan V, Šuštaršič B and Sirc A 2006 The use of soft magnetic composite materials in synchronous electric motor *J. Magn. Magn. Mater.* **304** e816–19
[2] Vázquez M and Hernando A 1996 A soft magnetic wire for sensor applications *J. Phys. D: Appl. Phys.* **29** 939
[3] Sato H, Tanaka T and Iwakami T 1992 New magnetic materials and their applicability to high-frequency transformers *Takaoka Rev.* **39** 40–3
[4] Georgilakis P, Hatziargyriou N, Paparigas D and Elefsiniotis S 2001 Effective use of magnetic materials in transformer manufacturing *J. Mater. Process. Technol.* **108** 209–12
[5] Sullivan C R and Sanders S R 1996 Design of microfabricated transformers and inductors for high-frequency power conversion *IEEE Trans. Power Electron.* **11** 228–38
[6] Sun N X and Wang S X 2000 Soft high saturation magnetization $(Fe_{0.7}Co_{0.3})_{1-x}N_x$ thin films for inductive write heads *IEEE Trans. Magn.* **36** 2506–8
[7] Yoshizawa Y, Oguma S and Yamauchi K 1988 New Fe-based soft magnetic alloys composed of ultrafine grain structure *J. Appl. Phys.* **64** 6044–6
[8] Kumasaka N, Saito N, Shiroishi Y, Shiiki K, Fujiwara H and Kudo M 1984 Magnetic properties of multilayered Fe–Si films *J. Appl. Phys.* **55** 2238–40
[9] Yin L F, Wei D H, Lei N, Zhou L H, Tian C S, Dong G S, Jin X F, Guo L P, Jia Q J and Wu R Q 2006 Magnetocrystalline anisotropy in permalloy revisited *Phys. Rev. Lett.* **97** 067203
[10] Haumer P, Hauser H, Fulmek P L and Bajalan D 2004 Hysteresis modeling of thin permalloy films and parameter interpretation *IEEE Trans. Magn.* **40** 2745–7
[11] Jiang H, Chen Y, Dang X and Krounbi M T Magnetically soft, high saturation magnetization laminates of iron-cobalt-nitrogen and iron-nickel *US Patent Specification* 7177117 B1
[12] Shokrollahi H and Janghorban K 2007 Soft magnetic composite materials (SMCs) *J. Mater. Process. Technol.* **189** 1–12
[13] Margeat O, Ciuculescu D, Lecante P, Respaud M, Amiens C and Chaudret B 2007 NiFe nanoparticles: a soft magnetic material? *Small* **3** 451–8
[14] Osaka T, Takai M, Hayashi K and Ohashi K 1998 A soft magnetic CoNiFe film with high saturation magnetic flux density and low coercivity *Nature* **392** 796–8

[15] Liu X, Miyao T, Fu Y and Morisako A 2006 Soft magnetic properties of FeCo films with Co underlayer *J. Magn. Magn. Mater.* **303** e201–4
[16] Inoue A, Shen B, Koshiba H, Kato H and Yavari A R 2003 Cobalt-based bulk glassy alloy with ultrahigh strength and soft magnetic properties *Nat. Mater.* **2** 661–3
[17] Roth S, Stoica M, Degmová J, Gaitzsch U, Eckert J and Schultz L 2006 Fe-based bulk amorphous soft magnetic materials *J. Magn. Magn. Mater.* **304** 192–6
[18] Fish G E 1990 Soft magnetic materials *Proc. IEEE* **78** 947–72
[19] Pan G and Du H 2003 (FeCo/Co-M)n soft magnetic multilayers with uniaxial anisotropy and very high saturation magnetization *J. Appl. Phys.* **93** 5498–502
[20] King A 2017 *Rare Earths and Other Critical Materials* (Ames, IA: Critical Materials Institute)
[21] Kim T K and Takahashi M 1972 New magnetic material having ultrahigh magnetic moment *Appl. Phys. Lett.* **20** 492–4
[22] Ji N, Osofsky M S, Lauter V, Allard L F, Li X, Jensen K L, Ambaye H, Lara-Curzio E and Wang J P 2011 Perpendicular magnetic anisotropy and high spin-polarization ratio in epitaxial Fe–N thin films *Phys. Rev.* B **84** 245310
[23] Jiang Y, Mehedi M Al, Fu E, Wang Y, Allard L F and Wang J-P 2016 Synthesis of $Fe_{16}N_2$ compound free-standing foils with 20 MGOe magnetic energy product by nitrogen ion-implantation *Sci. Rep.* **6** 25436
[24] Dementjev A P, De Graaf A, Van de Sanden M C M, Maslakov K I, Naumkin A V and Serov A A 2000 X-ray photoelectron spectroscopy reference data for identification of the C_3N_4 phase in carbon–nitrogen films *Diam. Relat. Mater.* **9** 1904–7
[25] Furlan A, Jansson U, Lu J, Hultman L and Magnuson M 2015 Structure and bonding in amorphous iron carbide thin films *J. Phys. Condens. Matter* **27** 45002
[26] Herbst J and Pinkerton F 1998 Law of approach to saturation for polycrystalline ferromagnets: remanent initial state *Phys. Rev.* B **57** 10733–9
[27] Uchida S, Kawakatsu T, Sekine A and Ukai T 2007 Magnetocrystalline anisotropy energies of $Fe_{16}N_2$ and $Fe_{16}C_2$ *J. Magn. Magn. Mater.* **310** 1796–8
[28] Takahashi M, Takahashi Y and Shoji H 2001 Magnetocrystalline anisotropy for α'-Fe–C and α'-Fe–N films *Magn. IEEE Trans.* **37** 2179–81
[29] Takahashi H, Igarashi M, Kaneko A, Miyajima H and Sugita Y 1999 Perpendicular uniaxial magnetic anisotropy of $Fe_{16}N_2$ (0 0 1) single crystal films grown by molecular beam epitaxy *IEEE Trans. Magn.* **35** 2982–4